Vol. 34 (2003) *ACTA PHYSICA POLONICA B* No 7

QUANTUM MAYER GRAPHS: APPLICATION TO BOSE AND COULOMB GASES*

Philippe A. Martin

Institute of Theoretical Physics, Swiss Federal School for Technology-Lausanne
CH-1015, Lausanne EPFL, Switzerland

(Received November 11, 2002)

The functional integral representation of quantum statistical mechanics by means of the Feynman–Kac formula leads to a classical-like description of the system. Point quantum particles are then described in terms of random loops (closed Brownian paths), and all techniques of classical statistical mechanics become available. One advantage of this formalism is that it is not perturbative with respect to the interaction strength, in contrast to the standard many-body perturbative treatment. We apply these ideas to the Coulomb gas by constructing an effective potential (the quantum analogue of the Debye potential) that incorporates both long distance collective screening effects as well as the short range quantum mechanical binding. For Bose systems, we show that mean field theory corresponds to summing all tree-graphs and investigate how to go beyond the mean field description.

PACS numbers: 05.30.–d, 71.45.–d

1. Introduction

The standard perturbative treatment of many particle systems relies on an expansion in the strength of the interparticle interaction. This leads to the familar Feynman diagrams of the many-body theory, see *e.g.* [1]. In some circumstances such an expansion is not appropriate, especially when the effect of the interaction is not analytic in the coupling constant. For instance, quantum mechanical binding in partially recombined plasmas, Bose condensation in interacting gases, as well as superconductivity cannot be described perturbatively.

---

[*] Presented at the XV Marian Smoluchowski Symposium on Statistical Physics, Zakopane, Poland, September 7–12, 2002.

Another possible small parameter in the system is the density or the fugacity: this leads to the virial expansion. However the traditionnal quantum virial expansion is cumbersome. We propose in these notes an alternative formalism that enables to benefit of the well developped classical tools of Mayer diagrammatic.

The point is that using the Feynman–Kac functional integral representation of the Gibbs weight together with the decomposition of permutations into cycles, the grand-canonical partition function of the quantum system takes the classical-like form of a gas of random loops (or "polymers"). A loop is a closed Brownian path originating at some point in space; it is an extended object that has a shape and carries a number of particles assimilated to internal degrees of freedom. In the auxillary space of loops, all techniques of classical statistical mechanics are at hand, in particular the very powerful and flexible Mayer diagrammatic techniques. From there we can easily come back to the calculation of quantities of interest for the original system of quantum particles. In fact this classical-like representation of the quantum system has been known in a form an another since a long time in various contexts, starting with the work of Ginibre on the convergence of the quantum virial expansion (see [2] and original references therein). It has also used to implement numerical simulations, see *e.g.* for Bose systems [3]. The present version has been derived and applied by Cornu [4] to Coulomb systems. Here we follow the definitions given in the review [5] where additionnal references can also be found. In Section 2 we give an essentially self contained derivation of the so called "magic formula" that dispays the partition of the quantum gas as that of a classical-like gas of loops. For simplicity we consider only one species of particles and the derivation is based on combinatorial properties of the permutation group. The generalisation to several species of particles can be found in [5] where another derivation is sketched in the framework of second quantization.

Section 3 is devoted to applications to the quantum plasma. We mainly formulate the analogue of the classical Debye–Hückel theory for quantum charges and indicates some striking consequences due to the quantum mechanical nature of the particles. In Section 4 we consider the Bose gas and show how the mean field limit can be recovered by a diagrammatic analysis.

2. The magic formula

We consider a system of N nonrelativisic bosonic or fermionic quantum particles enclosed in a box Λ and interacting by means of the two-body potential $V(\boldsymbol{r})$. The total Hamiltonian reads

$$H_N = \sum_{i=1}^{N} \frac{|\boldsymbol{p}_i|^2}{2m} + \sum_{i<j}^{N} V(\boldsymbol{r}_i - \boldsymbol{r}_j)\,, \tag{1}$$

where $|\boldsymbol{p}_i|^2 = -\hbar^2\Delta_i$, Δ_i is the Laplacian on $\Re^3$ with Dirichlet conditions at the boundary of Λ. The properties of the potential $V(\boldsymbol{r})$ will be specified in more detail in the applications.

The corresponding grand canonical partition function with inverse temperature $\beta = \frac{1}{k_{\mathrm{B}}T}$ and fugacity $z = \mathrm{e}^{\beta\mu}$ (μ is the chemical potential) is

$$\Xi_\Lambda = \sum_{N=0}^{\infty} \frac{z^N}{N!} \sum_{\pi} (\eta)^\pi f(\pi)\,, \tag{2}$$

where the second sum runs over all permutation π of the permutation group $\mathcal{S}_N$ of N elements. In (2) we have noted

$$f(\pi) = \int\limits_\Lambda d\boldsymbol{r}_1 \ldots \int\limits_\Lambda d\boldsymbol{r}_N \langle \boldsymbol{r}_1, \ldots, \boldsymbol{r}_N | \mathrm{e}^{-\beta H_\Lambda} U_\pi | \boldsymbol{r}_1, \ldots, \boldsymbol{r}_N \rangle \tag{3}$$

the configurational integral of the matrix elements of the Gibbs weight $\mathrm{e}^{-\beta H_\Lambda}$.

The operators U_π acts on the configurational kets as

$$U_\pi|\boldsymbol{r}_1, \ldots, \boldsymbol{r}_N\rangle = |\boldsymbol{r}_{\pi 1}, \ldots, \boldsymbol{r}_{\pi N}\rangle\,. \tag{4}$$

They form a unitary representation of the permutation group on the N particle states

$$U_{\pi_1} U_{\pi_2} = U_{\pi_1 \pi_2}\,, \qquad U_\pi^* = U_\pi^{-1} = U_{\pi^{-1}} \tag{5}$$

and $(\eta)^\pi$ is the signature of the permutation ($\eta = +1$ for bosons and $\eta = -1$ for fermions) . In a first step we consider in (2) the structure of sum on the function $f(\pi)$ defined on the permutation group $\mathcal{S}_N$.

2.1. Some facts on the permutation group

Each permutation π in $\mathcal{S}_N$ can be decomposed into k cycles of length q_i, $i = 1, \ldots, k$, with $k \leq N$, $\sum_{i=1}^k q_i = N$. We denote simply by $\mathcal{Q}$ the unordered set of integers

$$\mathcal{Q} = \{q_i,\, i = 1, \ldots, k,\, \sum_{i=1}^{k} q_i = N\} \tag{6}$$

and call it a cycle structure. For instance the permutation

$$\pi = \begin{pmatrix} 1\,2\,3\,4\,5\,6\,7 \\ 7\,5\,2\,6\,3\,4\,1 \end{pmatrix} = (1\,7)(2\,5\,3)(4\,6)$$

has the cycle structure $\mathcal{Q} = \{q_1 = 2,\, q_2 = 3,\, q_3 = 2\}$.

Two permutations π' and π'' having the same cycle structure $\mathcal{Q}$ are conjugate in $\mathcal{S}_{\mathcal{N}}$, that is there exists π such that

$$\pi'' = \pi^{-1}\pi'\pi\,. \tag{7}$$

Hence $\mathcal{S}_N$ is the disjoint union of equivalence classes of permutations having the same cycle structure. Let n_j be the number of cycles of length j in $\mathcal{Q}$, $n_j = 0, 1, \ldots, N$, $\sum_{n_j \geq 1} jn_j = N$ (in the above example, $n_2 = 2$, $n_3 = 1$, $n_j = 0, j \neq 2, 3$). Then the number of permutations that have the same cycle structure is [6] [1]

$$\mathcal{N}_{\mathcal{Q}} = \frac{1}{q_1 \ldots q_k} \frac{N!}{n_1! \ldots n_N!}\,. \tag{8}$$

Moreover the signature of a permutation

$$(\eta)^{\pi} = (\eta)^{\mathcal{Q}} = \prod_{i=1}^{k} \eta^{q_i - 1} \tag{9}$$

depends only on the cycle structure of π.

An important observation is that the same is true for $f(\pi)$ (3): it depends only on the cycle structure of π. Indeed if π' and π'' are conjugate, one has from (3), (5) and (7)

$$\begin{aligned} f(\pi'') &= \int_{\Lambda} d\boldsymbol{r}_1 \ldots \int_{\Lambda} d\boldsymbol{r}_N \langle \boldsymbol{r}_1, \ldots, \boldsymbol{r}_N | \mathrm{e}^{-\beta H_\Lambda} U_\pi^{-1} U_{\pi'} U_\pi | \boldsymbol{r}_1, \ldots, \boldsymbol{r}_N \rangle \\ &= \int_{\Lambda} d\boldsymbol{r}_1 \ldots \int_{\Lambda} d\boldsymbol{r}_N \langle \boldsymbol{r}_1, \ldots, \boldsymbol{r}_N | U_\pi^* \mathrm{e}^{-\beta H_\Lambda} U_{\pi'} U_\pi | \boldsymbol{r}_1, \ldots, \boldsymbol{r}_N \rangle \\ &= \int_{\Lambda} d\boldsymbol{r}_1 \ldots \int_{\Lambda} d\boldsymbol{r}_N \langle \boldsymbol{r}_{\pi_1}, \ldots, \boldsymbol{r}_{\pi_N} | \mathrm{e}^{-\beta_\Lambda} U_{\pi'} | \boldsymbol{r}_{\pi_1}, \ldots, \boldsymbol{r}_{\pi_N} \rangle = f(\pi'). \end{aligned} \tag{10}$$

We have used that H_Λ commutes with all permutation operators and relabelled the dummy integration variables to obtain the last equality.

Select a representative permutation $\bar{\pi}_{\mathcal{Q}}$ in the class $\mathcal{Q}$, for instance the canonical one that has numbers in increasing order (in our example,

---

[1] By convention $n! = 0$ when $n = 0$.

$\bar{\pi}_{\mathcal{Q}}$=(1,2)(3,4)(5,6,7)). Then in view of (9) and (10) the sum over permutations in (2) reduces to a sum over cycle structures

$$\begin{aligned}\sum_{\pi}(\eta)^{\pi}f(\pi) &= \sum_{\mathcal{Q}}\mathcal{N}_{\mathcal{Q}}(\eta)^{\mathcal{Q}}f(\bar{\pi}_{\mathcal{Q}})\\ &= \sum_{k=1}^{N}\sum_{q_1,\dots,q_k=1}^{\infty}\delta_{\sum_i^k q_i,N}\frac{n_1!\dots n_N!}{k!}\mathcal{N}_{\mathcal{Q}}(\eta)^{\mathcal{Q}}f(\bar{\pi}_{\mathcal{Q}})\\ &= N!\sum_{k=1}^{N}\frac{1}{k!}\sum_{q_1,\dots,q_k=1}^{\infty}\delta_{\sum_i^k q_i,N}\prod_{i=1}^{k}\frac{\eta^{q_i-1}}{q_i}f(\bar{\pi}_{(q_1,\dots,q_k)})\,. \qquad (11)\end{aligned}$$

In the second equality we have replaced the summation on cycle structures by a summation on ordered cycle lengths, which leads to an over counting compensated by the factor $n_1!\dots n_N!/k!$. The last equality follows from (8) and (9). Finally forming the grand canonical sum (2) removes the constraint of fixed N

$$\Xi_{\Lambda}=\sum_{k=0}^{\infty}\frac{1}{k!}\sum_{q_1,\dots,q_k=1}^{\infty}\prod_{i=1}^{k}\frac{\eta^{q_i-1}z^{q_i}}{q_i}f(\bar{\pi}_{(q_1,\dots,q_k)})\,. \qquad (12)$$

We have thus converted the particle number summation in the grand partition function to a sum on cycle numbers.

2.2. The Feynman–Kac representation

Let us first recall familiar ideas about the representation of the quantum mechanical statistical operator by the Feynman–Kac functional integral[2]. For sake of simplicity, we consider a single particle of mass m in three dimensions submitted to an external potential $\psi(\boldsymbol{r})$. According to the original path integration introduced by Feynman [7], the configurational matrix elements of the statistical operator associated with the one-particle Hamiltonian

$$H=-\frac{\hbar^2}{2m}\Delta+V, \qquad \Delta=\text{Laplacian in } \Re^3 \qquad (13)$$

read

$$\langle\boldsymbol{r}_1|\exp\left(-\beta\left(-\frac{\hbar^2}{2m}\Delta+\psi\right)\right)|\boldsymbol{r}_2\rangle=\sum_{\text{paths}}\exp\left(-\frac{1}{\hbar}S(\boldsymbol{r}(\cdot))\right)\,. \qquad (14)$$

---

[2] This subsection and the next one are essentially taken from Chaps. 4 and 5 in [5].

Here $S(\boldsymbol{r}(\cdot))$ is the classical action corresponding to the potential $-\psi$ (the Euclidean action)

$$S(\boldsymbol{r}(\cdot)) = \int\limits_0^{\beta\hbar} dt \left(\frac{m}{2}\left|\frac{d\boldsymbol{r}(t)}{dt}\right|^2 + \psi(\boldsymbol{r}(t))\right) \tag{15}$$

associated with the path $\boldsymbol{r}(t)$ starting from $\boldsymbol{r}_1$ at "time" $t=0$ and ending in $\boldsymbol{r}_2$ at "time" $\beta\hbar$. The summation in (14) runs over all such paths.

It is very useful to parameterize the path $\boldsymbol{r}(t)$ by dimensionless variables, making the change

$$\begin{aligned} s &= \frac{t}{\beta\hbar}\,, & 0 \leq s \leq 1 \\ \boldsymbol{r}_{1,2}(s) &= (1-s)\boldsymbol{r}_1 + s\boldsymbol{r}_2 + \lambda\boldsymbol{\xi}(s)\,, & \boldsymbol{\xi}(0) = \boldsymbol{\xi}(1) = 0\,, \end{aligned} \tag{16}$$

where

$$\lambda = \hbar\sqrt{\frac{\beta}{m}} \tag{17}$$

is the de Broglie thermal wave length. In (16) $\boldsymbol{\xi}(s)$ represents now a closed path, called the Brownian bridge, starting and returning to the origin within the "time" $s=1$. In terms of these dimensionless variables, the matrix element (14) can be written in the precise form [8]

$$\begin{aligned} \langle \boldsymbol{r}_1 \mid \exp\left(-\beta\left(-\frac{\hbar^2}{2m}\Delta + \psi\right)\right) \mid \boldsymbol{r}_2\rangle &= \left(\frac{1}{2\pi\lambda^2}\right)^{3/2} \exp\left(-\frac{|\boldsymbol{r}_1-\boldsymbol{r}_2|^2}{2\lambda^2}\right) \\ \times \int D(\boldsymbol{\xi}) \exp &\left(-\beta\int\limits_0^1 ds V((1-s)\boldsymbol{r}_1 + s\boldsymbol{r}_2 + \lambda\boldsymbol{\xi}(s))\right)\,. \end{aligned} \tag{18}$$

In (18) $D(\boldsymbol{\xi})$ is a Gaussian measure (the Brownian bridge measure) with weight formally represented by $\exp\left(-\frac{1}{2}\int_0^1\left|\frac{d\boldsymbol{\xi}(s)}{ds}\right|^2\right)$. It is normalized to 1, has zero mean and is entirely defined by its covariance

$$\int D(\boldsymbol{\xi})\xi_\mu(s_1)\xi_\nu(s_2) = \delta_{\mu,\nu}(\min(s_1,\, s_2) - s_1 s_2)\,, \tag{19}$$

where $\xi_\mu(s)$ are the Cartesian coordinates of $\boldsymbol{\xi}(s)$.

The representation (18) has the advantage that physical parameters $\boldsymbol{r}_1$, $\boldsymbol{r}_2$, β, $\hbar$, λ appear explicitly in the formula; λ measures the extent of the quantum fluctuation. In particular if λ is set equal to zero in the diagonal matrix element one recovers the classical Boltzmann weight.

The extension to the many particle system is straightforward. To each particle is associated a path $\boldsymbol{\xi}_i(s)$ The paths are distributed with independent Gaussian measures $D(\boldsymbol{\xi}_i)$, $i = 1, \ldots, N$, so that the matrix element in (3) reads

$$\langle \boldsymbol{r}_1, \ldots, \boldsymbol{r}_N | \exp(-\beta H_\Lambda) | \boldsymbol{r}_{\pi_1}, \ldots, \boldsymbol{r}_{\pi_N} \rangle = \prod_{i=1}^{N} \left(\frac{1}{2\pi\lambda^2} \right)^{3/2}$$

$$\times \exp\left(-\frac{|\boldsymbol{r}_i - \boldsymbol{r}_{\pi_i}|^2}{2\lambda^2} \right) \int \prod_{i=1}^{N} D(\boldsymbol{\xi}_i)$$

$$\times \exp\left(-\beta \sum_{i<j}^{N} \int_0^1 ds V(\boldsymbol{r}_{i,\pi_i}(s) - \boldsymbol{r}_{j,\pi_j}(s)) \right). \tag{20}$$

We now introduce this representation in the formula (12) to obtain the gas of loops.

2.3. The statistical mechanics of loops

In the interaction energy in (20) we group all the particle belonging to a given cycle of length q in $\bar{\pi}$, say the particles $1, 2, \ldots, q$. The corresponding collection of paths

$$\boldsymbol{r}_{i,i+1}(s_i) = (1 - s_i)\boldsymbol{r}_i + s_i\boldsymbol{r}_{i+1} + \lambda\boldsymbol{\xi}(s_i), \quad i = 1, \ldots, q, \quad (q + 1 \equiv 1)$$

are joined together to from again a closed Brownwian path, the random loop

$$\boldsymbol{R}(s) = \boldsymbol{r}_{i,i+1}(s_i), \quad i - 1 \leq s < i\,. \tag{21}$$

The loop is now parametrized by the single time parameter s running from 0 to q by setting $s_i = s - [s]$, $i - 1 \leq s < i$ where $[s]$ is the integer part of s, see Fig. 1.

One can then locate the loop at $\boldsymbol{R}$ by selecting the position of one of the particles, say $\boldsymbol{r}_1 = \boldsymbol{R}$, and write

$$\boldsymbol{R}(s) = \boldsymbol{R} + \lambda\boldsymbol{X}(s), \quad \boldsymbol{X}(0) = \boldsymbol{X}(q) = 0\,. \tag{22}$$

Hence the particles are located at the points

$$\boldsymbol{r}_k = \boldsymbol{R} + \lambda\boldsymbol{X}(k-1), \quad k = 1, \ldots, q\,. \tag{23}$$

In (22), $\boldsymbol{X}(s)$ is again a dimensionless Brownian bridge starting and returning to the origin within the time q. Its normalized Gaussian measure $D_q(\boldsymbol{X})$

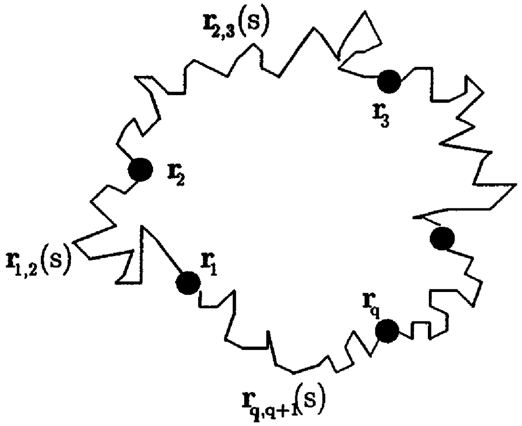

Fig. 1. A q particle loop.

is the composition of that of the q open filaments that constitute the loop (see (18))

$$D_q(\boldsymbol{X}) = (2\pi q)^{3/2} \prod_{k=1}^{q} \frac{\exp\left(-\frac{1}{2}(\boldsymbol{X}_{k+1} - \boldsymbol{X}_k)^2\right)}{(2\pi)^{3/2}} d\boldsymbol{X}_2 \ldots d\boldsymbol{X}_q D(\boldsymbol{\xi}_1) \ldots D(\boldsymbol{\xi}_q), \tag{24}$$

where one sets $\boldsymbol{X}_1 = \boldsymbol{X}_{q+1} = 0$. One can calculate its covariance from the definitions (19), (21) and (22)

$$\int D_q(\boldsymbol{X}) X_\mu(s_1) X_\nu(s_2) = \delta_{\mu\nu} q \left[\min\left(\frac{s_1}{q}, \frac{s_2}{q}\right) - \frac{s_1}{q}\frac{s_2}{q}\right]. \tag{25}$$

Thus a loop $\boldsymbol{R}(s)$ is characterized by its location in space, the number q of particle it carries and its shape $\boldsymbol{X}(s)$. We denote collectively the set of parameters

$$\mathcal{L} = \{\ \boldsymbol{R},\ q,\ \boldsymbol{X}(\cdot)\ \} \tag{26}$$

and consider $\mathcal{L}$ as a point in the phase space of loops. The parameters q and $\boldsymbol{X}(\cdot)$ can be thought as the internal degrees of freedom of a loop located at $\boldsymbol{R}$, and the phase space integration is defined as

$$d\mathcal{L} \ldots = \int d\boldsymbol{R} \sum_{q=1}^{\infty} \int D_q(\boldsymbol{X}) \ldots . \tag{27}$$

We select in (20) all the pair interactions of particles belonging to the same loop to constitute the self energy of the loop $U(\mathcal{L})$. According to the definitions (21) and (22) it can be written as

$$U(\mathcal{L}) = \frac{1}{2}\int\limits_0^q ds_1 \int\limits_o^q ds_2 \left(1 - \delta_{[s_1],[s_2]}\right) \tilde{\delta}(s_1 - s_2) V(\lambda(\boldsymbol{X}(s_1) - \boldsymbol{X}(s_2))) \,. \quad (28)$$

The periodic delta function

$$\tilde{\delta}(s) = \sum_{n=-\infty}^{\infty} \mathrm{e}^{2i\pi n s} \quad (29)$$

assures the equal time interaction condition that occurs in the Feynman-Kac representation (20). The term involving the Kronecker symbol $\delta_{[s_1],[s_2]}$ substracts out in (28) the self energy of the particles $qV(0)$.

All quantities pertaining to a single loop in (20) and (12) are now collected into the loop activity

$$z(\mathcal{L}) = \frac{(\eta)^{q-1}}{q} \frac{\exp(\beta\mu q)}{(2\pi q \lambda^2)^{3/2}} \exp(-\beta U(\mathcal{L})) \,. \quad (30)$$

Finally, one must take into account the remaining interaction potentials in (20) that couple particles belonging to different loops, namely

$$U(\mathcal{L}_1, \ldots, \mathcal{L}_k) = \sum_{1=i<j}^{k} V(\mathcal{L}_i, \mathcal{L}_j) \quad (31)$$

with the loop pair potential

$$V(\mathcal{L}_1, \mathcal{L}_2) = \int\limits_0^{q_1} ds_1 \int\limits_0^{q_2} ds_2 \tilde{\delta}(s_1 - s_2) V(\boldsymbol{R}_1 + \lambda\boldsymbol{X}(s_1) - \boldsymbol{R}_2 - \lambda\boldsymbol{X}(s_2)) \,. \quad (32)$$

Then putting all definitions together leads to the final formula for the partition function Ξ_Λ (12) (the "magic formula")

$$\Xi_\Lambda = \sum_{k=0}^{\infty} \frac{1}{k!} \int \prod_{i=1}^{k} d\mathcal{L}_i z(\mathcal{L}_i) \exp(-\beta U(\mathcal{L}_1, \ldots, \mathcal{L}_k)) \,. \quad (33)$$

We call the system defined by the relations (25) to (33) the "system of loops" or "system of polymers" associated to the quantum mechanical many-body problem. Although the so defined statistical mechanics of polymers has a classical structure, one should be aware that the polymers do not have the genuine classical pairwise interaction between their elements which would read

$$V_{\text{classical}}(\mathcal{L}_1,\mathcal{L}_2)=\int\limits_0^{q_1}ds_1\int\limits_0^{q_2}ds_2V(\boldsymbol{R}_1+\lambda\boldsymbol{X}(s_1)-\boldsymbol{R}_2-\lambda\boldsymbol{X}(s_2)) \qquad (34)$$

instead of (32). The "quantum polymer" interaction (32) is constrained by the equal time condition $\tilde{\delta}(s_1-s_2)$ which is of purely quantum origin.

At this point one can benefit of the classical-like structure of the partition function (33) to use the available tools of classical statistical mechanics in the space of polymers, in particular the Mayer diagrammatic [15]. Labelled Mayer graphs $\mathit{\Gamma}_n$ consist of n vertices (i), $i=1,\dots,n$, connected by bonds $f(i,j)$. In the space of loops, a vertex (i) is labelled by the loop variable $\mathcal{L}_i$ and receives a weight given by the activity $z(\mathcal{L}_i)$ (30). The bond linking the vertices (i) and (j) is defined by

$$f(i,j)=\exp(-\beta V(\mathcal{L}_i,\mathcal{L}_j))-1 \qquad (35)$$

with $V(\mathcal{L}_i,\mathcal{L}_j)$ the loop-loop interaction (32). From there one can obtain all quantities of interest according to the standard rules of Mayer diagrammatic. As an example, the density of loops $\rho_{\text{loop}}(\mathcal{L})$ is given by the standard expansion

$$\rho_{\text{loop}}(\mathcal{L}_1)=\sum_{n=1}^{\infty}\frac{1}{(n-1)!}\int d\mathcal{L}_2\dots d\mathcal{L}_n z(\mathcal{L}_1)z(\mathcal{L}_2)\dots z(\mathcal{L}_n)u(\mathcal{L}_1,\mathcal{L}_2,\dots,\mathcal{L}_n), \qquad (36)$$

where

$$u(\mathcal{L}_1,\mathcal{L}_2,\dots,\mathcal{L}_n)=\sum_{\mathit{\Gamma}_n}\prod_{(i,j)\in\mathit{\Gamma}_n}f(i,j) \qquad (37)$$

is the Ursell function. The sum runs on all labelled connected graphs $\mathit{\Gamma}_n$ with n vertices. To obtain the low fugacity expansion of the particle density ρ from the loop density, we have to sum $\rho_{\text{loop}}(\mathcal{L})$ on the internal variables of $\mathcal{L}$,

$$\rho=\sum_{q=1}^{\infty}q\int D_q(\boldsymbol{X})\rho_{\text{loop}}(q,\boldsymbol{X}) \qquad (38)$$

the additional q factor taking into account that the loop $\mathcal{L}$ carries q particles. Higher order loop correlation functions can as well be written in terms of their Mayer expansions and the way to obtain the corresponding particle correlations is clarified for instance in the appendix D of [9].

3. Quantum plasma

We apply the formalism to the study of the screening mechanisms in a plasma of quantum mechanical charges. The system consists of $\mathcal{S}$ species of quantum particles with charges e_α, $\alpha = 1, \ldots, \mathcal{S}$, interacting with the Coulomb potential $e_{\alpha_1} e_{\alpha_2} \frac{1}{|\boldsymbol{r}_1 - \boldsymbol{r}_2|}$. In the polymer representation, this Coulomb gas is isomorphic to a system of charged fluctuating wires; the loop variable $\mathcal{L}$ includes now the additional index α that specifies the type of associated charges [3].

For classical charges, one knows that in the plasma the long range of the Coulomb potential is reduced because of screening: a given charge surrounds itself by a cloud of charges of opposite sign that cancels the Coulombic tail $|\boldsymbol{r}|^{-1}$ by neutrality. This replaces the bare Coulomb potential by an effective short range potential $V^{\rm eff}(\boldsymbol{r})$ in the medium. In the mean field theory scheme of Debye and Hückel, one has

$$\begin{aligned} V_{\rm D}^{\rm eff}(\boldsymbol{r}) &= \frac{{\rm e}^{-\kappa_{\rm D} r}}{r}, \quad r = |\boldsymbol{r}|, \\ \tilde{V}_{\rm D}^{\rm eff}(\boldsymbol{k}) &= \frac{4\pi}{k^2 + \kappa_{\rm D}^2}, \quad k = |\boldsymbol{k}|, \end{aligned} \tag{39}$$

where the second line gives the Fourier representation and

$$\kappa_{\rm D}^{-1} = (4\pi\beta \sum_\alpha z_\alpha e_\alpha^2)^{-1/2} \tag{40}$$

is the Debye screening length ($z_\alpha = {\rm e}^{\beta\mu_\alpha}$ and μ_α are the fugacity and the chemical potential of particles of species α). In the diagrammatic language, $V^{\rm eff}(\boldsymbol{r})$ is obtained as the chain summation of Mayer graphs with linearized bonds $f^{(\ell)}(i,j) = -\beta e_{\alpha_i} e_{\alpha_j} \frac{1}{|\boldsymbol{r}_i - \boldsymbol{r}_j|}$, see Fig. 2.

Fig. 2. The effective chain potential.

The same procedure can be applied to the quantum plasma by summing the chains of quantum Mayer graphs in the space of loops: this provides an effective loop-loop interaction which is the quantum analogue of the classical Debye potential. To condense the notation we set $\mathcal{L} = \{\boldsymbol{R}, \chi\}$ with $\chi = \{\alpha,\ q,\ \boldsymbol{X}\}$ denoting the set of internal degrees of freedom of the loop. The

---

[3] If particles have spins, the spin degeneracy is included in the loop activity $z(\mathcal{L})$.

result of the quantum mechanical chain summation is found to be in Fourier representation [9]

$$\begin{aligned}\tilde{V}^{\mathrm{eff}}(\boldsymbol{k},\chi_a,\chi_b) &= \int_0^{q_a} ds_a \int_0^{q_b} ds_b\, \mathrm{e}^{i\boldsymbol{k}\cdot[\lambda_a \boldsymbol{X}_a(s_a)-\lambda_b \boldsymbol{X}_b(s_b)]}\\ &\quad\times \sum_{n=-\infty}^{\infty} \frac{4\pi}{k^2+\kappa^2(k,n)} \mathrm{e}^{-2i\pi n(s_a-s_b)}.\end{aligned} \tag{41}$$

where the "screening coefficients" $\kappa^2(k,n)$ are given by

$$\kappa^2(k,n) = 4\pi\beta \sum_\alpha e_\alpha^2 \sum_q \int D(\boldsymbol{X})\, z(\chi) \left| \int_0^q ds\, \mathrm{e}^{i\boldsymbol{k}\cdot\lambda_\alpha \boldsymbol{X}(s)} \mathrm{e}^{2i\pi n s} \right|^2 \tag{42}$$

with λ_α the thermal wave length of the particle of species α and $z(\chi)$ the activity (30) of the loop. Although fermionic activities can be negative, the coefficients $\kappa^2(k,n)$ can be shown to be positive when the density is low enough. One notes on (42) that in the classical limit (*i.e.* $q=1$, Boltzmann statistics, and $\lambda_\alpha=0$), $\kappa^2(k,n)$ vanishes for $n \neq 0$ whereas $\kappa^2(k,0)$ reduces to κ_{D} and hence one recovers the classical Debye potential (40). In general one has $\lim_{k\to 0}\kappa^2(k,0) = \kappa_{\mathrm{D}}^2(1+\mathcal{O}(z)) \neq 0$ but if $n \neq 0$, $\kappa^2(k,n)=\mathcal{O}(k^2)$ vanishes as $k \to 0$. This shows that in the sum in (41) the term $n=0$ is regular at $k=0$ and is thus responsible for classical screening, but the $n \neq 0$ terms have a k^{-2} singularity that will cause an algebraic tail at long distances (see (43) bellow).

The formula (41) is considerably more complicated than the simple classical Debye potential (39) since it embodies the effects of the quantum fluctuations. However in the low density ($z \ll 1$) and weakly degenerate ($\lambda\kappa_{\mathrm{D}} \ll 1$) regime $\tilde{V}^{\mathrm{eff}}(\boldsymbol{k},\chi_a,\chi_b)$ has a physically clear meaning depending on various spatial scales (for a detailed analysis see [9]). Several applications of the formalism of quantum Mayer graphs to quantum plasmas and more references are found in the review [5].

Long distance behaviour, $r \gg \kappa_{\mathrm{D}}^{-1}$

At very large distances, the decay is dominated by the multipole interactions between charged loops of arbitrary shapes. A loop $\mathcal{L}$ carries an instantaneous dipole moment $e_\alpha\lambda_\alpha\boldsymbol{X}(s)$ so that the asymptotic behaviour is that of a dipole-dipole interaction potential

$$V^{\mathrm{eff}}(\boldsymbol{r},\chi_a,\chi_b) \sim \int\limits_0^{q_a} ds_a \int\limits_0^{q_b} ds_b (1-\tilde{\delta}(s_a-s_b))(\lambda_a \boldsymbol{X}(s_a)\cdot\nabla)(\lambda_b \boldsymbol{X}(s_b)\cdot\nabla)\frac{1}{r} \tag{43}$$

as $r=|\boldsymbol{r}_a-\boldsymbol{r}_b|\to\infty$. One notes that monopoles are screened, *i.e.* charge-charge and charge-dipole terms do not occur in the asymptotic form (43) so that the bare Coulombic decay r^{-1} is only reduced in the plasma to a r^{-3} decay caracteristic for dipole interaction. This is a feature due to intrinsic quantum fluctuations: the latter are at the origin of multipole forces that cannot be screened in the quantum plasma. These residual multipole forces give rise to an algebraic decay of the particle correlations which is of the form (in a spatially homogeneous plasma) [10]

$$\rho_{ab}(\boldsymbol{r}_a,\boldsymbol{r}_b)-\rho_a\rho_b \sim \frac{A_{ab}}{|\boldsymbol{r}_a-\boldsymbol{r}_b|^6}, \quad |\boldsymbol{r}_a-\boldsymbol{r}_b|\to\infty\,, \tag{44}$$

where $\rho_{ab}(\boldsymbol{r}_a,\boldsymbol{r}_b)$ is the correlation function for particles of species a and b, and the coefficient A_{ab} depends of the thermodynamical parameters of the plasma phase. The reduction of the dipole decay r^{-3} (43) to the van der Waals like decay r^{-6} is due to the spherically symetrical average over loop dipoles when integrating the internal degrees of freedom of the loops.

It is remarkable that in the electron–proton plasma the coefficients A_{ab} can be explicitly calculated at the lowest order in density [11]. The all have the common value

$$A_{ee}=A_{ep}=A_{pp}=\rho^2\frac{\hbar^4\beta^4e^4}{960}\left(\frac{1}{m_e}+\frac{1}{m_p}\right)^2 . \tag{45}$$

One finds also that the correlation of a particle ar $\boldsymbol{r}_a$ with the total charge at $\boldsymbol{r}_b$ decays as $|\boldsymbol{r}_a-\boldsymbol{r}_b|^{-8}$ and the charge-charge correlation decays as $|\boldsymbol{r}_a-\boldsymbol{r}_b|^{-10}$. The main point is that correlations of quantum charges never show the exponential decay predicted by the classical Debye–Hückel theory (39), but have various types of algebraic decays generated by the loop fluctuations in the polymer representation of the plasma.

Intermediate distances, $r\sim\kappa_{\mathrm{D}}^{-1}$

The algebraic tail (43) (due to the singular $n\neq 0$ terms in (41)) is now of order $\lambda^2 r^{-3}\sim\lambda^2\kappa_{\mathrm{D}}^3$ and has to be compared to the contribution of the $n=0$ term. Replacing $\kappa^2(k,0)$ by κ_{D}^2 we see that this term is the classical screened Debye potential (39) between loops, which reads in configuration space

$$\begin{aligned} V_{\mathrm{D}}^{\mathrm{eff}}(\boldsymbol{r},\chi_a,\chi_b) &= \int_0^{q_a} ds_a \int_0^{q_b} ds_b \frac{\mathrm{e}^{-\kappa_{\mathrm{D}}|\boldsymbol{r}+\lambda_a \boldsymbol{X}_a(s_a)-\lambda_b \boldsymbol{X}_b(s_b)|}}{|\boldsymbol{r}+\lambda_a \boldsymbol{X}_a(s_a)-\lambda_b \boldsymbol{X}_b(s_b)|} \\ &\sim q_a q_b \frac{\mathrm{e}^{-\kappa_{\mathrm{D}} r}}{r}, \quad r \sim \kappa_{\mathrm{D}}^{-1}, \end{aligned} \tag{46}$$

where in the second line we have neglected terms of the order of $\lambda\kappa_{\mathrm{D}}$. In this range the contribution of the tail $\lambda^2 r^{-3}$ is $(\lambda\kappa_{\mathrm{D}})^2$ smaller than $V_{\mathrm{D}}^{\mathrm{eff}}(\boldsymbol{r},\chi_a,\chi_b)$ One concludes that on the scale $r \sim \kappa_{\mathrm{D}}^{-1}$ the effective loop-loop potential behaves as the standard Debye potential that describes collective screening effects.

Short distances, $r \ll \kappa_{\mathrm{D}}^{-1}$

If the distance between loops is very short compared to the Debye length, no screening effects take place and one finds that the effective potential reduces (up to a constant) to the bare loop-loop Coulomb potential

$$V^{\mathrm{eff}}(\boldsymbol{r},\chi_a,\chi_b) \sim \int_0^{q_a} ds_a \int_0^{q_b} ds_b \frac{1}{|\boldsymbol{r}+\lambda_a \boldsymbol{X}_a(s_a)-\lambda_b \boldsymbol{X}_b(s_b)|} - q_a q_b \kappa_{\mathrm{D}}, \quad r \to 0\,. \tag{47}$$

This will account for the quantum mechanical binding, which occurs at distances of the order of the Bohr radius $a_{\mathrm{B}} \ll \kappa_{\mathrm{D}}^{-1}$ and so gives the posssibility to describe recombination processes in the plasma (formation of atoms and molecules). The effective potential defined in (41) incorporates in a single function all the basic phenomena that screen the interaction of quantum charges at long, intermediate and short distances. In particular, after a reorganisation of the Mayer diagrammatic suitable to treat recombination problems, it enables to treat in a fully consistent way the corrections to the equation of state of ideal gases in the Saha regime. It can also be used to derive the first corrections to the van der Waals forces between atoms and molecules in a low density medium. These applications are the subject of a number of papers in preparation [12] .

4. Bose gas

Following the recent observation of Bose condensation of cold atoms in traps [13], there are strong motivations for a better understanding of the mechanism of this phase transition. We show how to recover the mean field theory of the homogeneous Bose gas by means of diagrammatic summation and discuss the mathematical problems that arise when one wants to extend the analysis beyond mean field.

It is well known that the van der Waals theory of the liquid-gas transition is obtained in the limit of a weak long range pair potential [14]

$$V_\gamma(\boldsymbol{r}) = \gamma^3 V(\gamma \boldsymbol{r}) \tag{48}$$

as $\gamma \to 0$ where $V(\boldsymbol{r})$ is a fixed potential with finite total integral $\int d\boldsymbol{r} V(\boldsymbol{r}) \equiv a < \infty$. In order to describe the liquid gas transition one needs a strong local repusion between the particles and $V_\gamma(\boldsymbol{r})$ only represents the long range attractive part of the interaction. For bosons the situation is different since the condensation phenomenon is already present in the free gas, the issue being to see whether the transition survives the introduction of an interaction. To assure thermodynamic stability, we assume that both the potential $V(\boldsymbol{r}) \geq 0$ and its Fourier transform $\tilde{V}(\boldsymbol{k}) \geq 0$ are positive.

The mean field equation is a self consistent relation that determines the grand canonical density $\rho(\mu)$ as function of the chemical potential μ

$$\rho(\mu) = \rho_0(\mu - a\rho(\mu))\,. \tag{49}$$

In (49)

$$\rho_0(\mu) = \frac{1}{(2\pi\lambda^2)^{3/2}} \sum_{q=1}^{\infty} \frac{\mathrm{e}^{\beta\mu q}}{q^{3/2}} \tag{50}$$

is the well known formula [15] for the grand canonical density of the free gas and

$$\lambda = \hbar\sqrt{\beta/m} \tag{51}$$

is the thermal wave length.

The series (50) converges for $\mu \leq 0$ so that the self consistent equation (49) is meaningful whenever $\mu - a\rho(\mu) \leq 0$, namely for $\mu \leq \mu_c$. The critical chemical potential μ_c is defined by $\mu_c - a\rho(\mu_c) = 0$, thus μ_c has the value $\mu_c = a\rho_{0,c}$ where $\rho_{0,c} = \rho_0(\mu = 0)$ is the critical density of the free gas.

The equation (49) has been rigorously derived in the limit $\gamma \to 0$ (where the range of the potential (48) extends to infinity) in a number of works [16–18] and is also known that its solution can be extended above the critical chemical potential as $\rho(\mu) = \mu/a$, $\mu > \mu_c$.

To establish equation (49) in the van der Waals limit in the diagrammatic language, let us first single out the dominant contributions of bond and vertices as $\gamma \to \infty$.

The contributions of order $\mathcal{O}(1)$ in γ of the scaled potential $\gamma^3 V(\gamma \boldsymbol{r})$ will come from the linarized bond $f_\gamma(i,j) \sim f_\gamma^{(\ell)}(i,j) \equiv -\beta V_\gamma(i,j)$ which reads (see (32))

$$f_\gamma^{(\ell)}(i,j) = -\beta\gamma^3 \int_0^{q_i} ds_i \int_0^{q_j} ds_j \tilde{\delta}(s_i - s_j) V(\gamma(\boldsymbol{R}_i - \boldsymbol{R}_j) + \gamma\lambda(\boldsymbol{X}_i(s_i) - \boldsymbol{X}_j(s_j)))\,. \tag{52}$$

This bond will give a contribution of order $\mathcal{O}(1)$ once integrated on one of the loop position $\boldsymbol{R}_i$ or $\boldsymbol{R}_j$ since by scaling its total spatial integral

$$\int d\boldsymbol{R}_j f_\gamma^{(\ell)}(i,j) = -\beta a q_i q_j \tag{53}$$

is independant of γ. In the activity (30) we simply disregard the self energy $U_\gamma(\mathcal{L})$ since the latter is $\mathcal{O}(\gamma^3)$ and approximate

$$z(\mathcal{L}) \sim z^{(0)}(q) \equiv \frac{z^q}{q(2\pi q\lambda^2)^{3/2}}\,. \tag{54}$$

The point is now that the mean field equation results of the summation of all tree graphs with bonds (52) and vertices (54)[4]. Consider indeed a rooted tree graph T_{n+1} with vertices $(0,1,\dots,n)$ for which the root point is of degree 1 (0 is the label of the root point) [5]. Hence the root point is linked to the rest of the graph by a single bond, say $f^{(\ell)}(0,1)$. Call T_n the subgraph of T_{n+1} with vertices $(1,2,\dots,n)$ and $t_n(\mathcal{L}_1)$ the value of this subgraph once integrated on the vertices $2,\dots,n$. Then the value $t_{n+1}(\mathcal{L}_0)$ of the rooted graph T_{n+1} is

$$t_{n+1}(\mathcal{L}_0) = -\beta z^{(0)}(q_0)\int d\mathcal{L}_1 V_\gamma(\mathcal{L}_0,\mathcal{L}_1)t_n(\mathcal{L}_1)\,. \tag{55}$$

Because of translation invariance $t_n(\mathcal{L}_1) = t_n(q_1,\boldsymbol{X}_1)$ does not depend on the position $\boldsymbol{R}_1$ of the loop $\mathcal{L}_1$. Thus the spatial integration $\boldsymbol{R}_1$ can be performed on $V_\gamma(\mathcal{L}_0,\mathcal{L}_1)$ as in (53) so that

$$nt_{n+1}(\mathcal{L}_0) = z^{(0)}(q_0)(-\beta a q_0)\left[\sum_{q_1=1}^{\infty} q_1\int D_{q_1}(\boldsymbol{X}_1)nt_n(q_1,\boldsymbol{X}_1)\right]\,. \tag{56}$$

According to (38) the quantity in the bracket is precisely the contribution to the particle density $\rho_{\text{tree}}(\mu)$ of the graph T_n[6]. Therefore the sum of all indexed tree graphs having a root point of degree 1 is

$$z^{(0)}(q_0)(-\beta a q_0\rho_{\text{tree}}(\mu))\,.$$

The sum of all tree graphs with root point of degree n is

$$z^{(0)}(q_0)(-\beta v q_0\rho_{\text{tree}}(\mu))^n/n!$$

---

[4] A tree is a Mayer graph without cycles.

[5] The degree of a point is the number of lines incident at this point.

[6] The additional factor n in (56) occurs because the root point 0 can be linked to any of the n vertices of T_n.

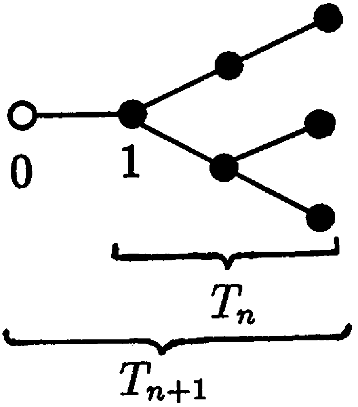

Fig. 3. A rooted tree graph with subgraph T_n.

(the factor $1/n!$ takes care of the fact that the labelling of vertices belonging to the different branches attached to the root point can be permuted without giving rise to new Mayer graphs). Finally, summing on all trees rooted at the point 0 gives the density of loops. To obtain the particle density we still have to sum on the internal variables $q_0, \boldsymbol{X}_0$ of the root loop with a factor q_0 according to (38). Hence introducing (54) yields

$$\begin{aligned}\rho_{\text{tree}}(\mu) &= \sum_{n=0}^{\infty} \frac{q_0 z^{(0)}(q_0)}{n!} \left(-\beta a q_0 \rho_{\text{tree}}(\mu)\right)^n \\ &= \sum_{q_0=1}^{\infty} \frac{\exp(\beta(\mu - a\rho_{\text{tree}}(\mu)))}{(2\pi q_0 \lambda^2)^{3/2}} \\ &= \rho_0(\mu - a\rho_{\text{tree}}(\mu)) ,\end{aligned} \tag{57}$$

which is the mean field equation (49). One has of course to prove that all the neglected terms (the non linear part of the bond $f_\gamma(i,j)$ and the graphs with cycles) do not contribute as $\gamma \to 0$, see [19].

The question now arises to investigate the first corrections to the mean field theory when γ is not driven to the limit but kept small. A first step in this direction is provided by a generalization of the mean field equation valid for the interacting gas [19]

$$\rho(\mu) = F(\mu - a\rho(\mu)) . \tag{58}$$

The difference with (49) is that here $F(\mu)$ contains the full information on the interacting gas. It is defined in the diagrammatic of loops as the sum of all irreducible Mayer graphs. The basic bond

$$f(i,j) = f^{(\ell}(i,j) + f^{(n\ell)}(i,j)$$

is decomposed into two new bonds

$$f^{(\ell)}(i,j) = -\beta V(i,j)$$

and

$$f^{(n\ell)}(i,j) = \mathrm{e}^{-\beta V(i,j)} - 1 + \beta V(i,j)\,.$$

Then a graph is said irreducible if it cannot be disconnected by cutting a linear interaction bond $f^{(\ell)}(i,j)$. One can show that the series of these graphs is convergent when the chemical potential is sufficiently negative (*i.e.* at sufficiently low density) so that equation (58) is meaningful in this regime. Moreover, as expected, $\lim_{\gamma\to 0} F_\gamma(\mu) = \rho_0(\mu)$ when the scaling parameter γ is introduced in the potential.

In order to see what is the nature of the problems involved in an analysis that goes beyond mean field let us consider the simplest irreducible diagram which is the single root vertex with activity $z(\boldsymbol{\mathcal{L}})$. Its contribution to $F(\mu)$ is according to (38) and (30) is

$$\begin{aligned} F^{(0)}(\mu) &= \sum_{q=1}^{\infty} q \int D_q(\boldsymbol{X}) z(\boldsymbol{\mathcal{L}}) \\ &= \frac{1}{(2\pi\lambda^2)^{3/2}} \sum_{q=1}^{\infty} \frac{\mathrm{e}^{\beta\mu q}}{q^{3/2}} \kappa(q)\,. \end{aligned} \tag{59}$$

Here we have introduced the partition function (normalized to 1)

$$\kappa(q) = \int D_q(\boldsymbol{X}) \mathrm{e}^{-\beta U(q,\boldsymbol{X})} \tag{60}$$

of a single closed polymer having the repulsive energy (28). Comparing (59) to (50) we see that the radius of convergence of the sum is now determined by the asymptotic behaviour of $\kappa(q)$ as $q \to \infty$. This radius will in turn determine a critical chemical potential renormalized by the interaction. It is firmly established, although not rigorously proved, that the normalized partition $\kappa_{\mathrm{cl}}(q)$ function of a single classical self repelling closed polymer with interaction (34) behaves (in three dimensions) as [20]

$$\kappa_{\mathrm{cl}}(q) \sim C \frac{\mathrm{e}^{-\beta A q}}{q^{3(\nu_{\mathrm{pol}}-1/2)}}\,, \quad q \to \infty\,, \tag{61}$$

where A is a constant depending of the choice of the potential $V(\boldsymbol{r})$ and $\nu_{\rm pol} = 0,589$ is the universal critical exponent for a swollen polymer. It is apparently not known at the moment if a similar behaviour holds for the "quantum polymers" occuring in the representation of the Bose gas. In addition one has also to deal with higher order irreducible graphs with cycles and bonds $f^{(n\ell)}(i,j)$ that involve pair interactions between different polymers. These questions are under investigation and we believe that they suggest interesting problems and analogies between the description of the Bose phase transition and polymer theories.

REFERENCES

[1] A. Fetter, J.D. Walecka, *Quantum Theory of Many Particle Systems*, McGraw-Hill, 1971.

[2] J. Ginibre, "Some applications of functional integration in statistical mechanics", *Statistical Mechanics and Quantum Field Theory*, C. DeWitt, R. Stora, eds, Les Houches, Gordon and Breach, 1971, p. 327.

[3] D.M. Ceperley, *Rev. Mod. Phys.* **67**, 279 (1995).

[4] F. Cornu, *Phys. Rev.* **E53**, 4562 (1996).

[5] D. Brydges, Ph.A. Martin, *J. Stat. Phys.* **96**, 1163 (1999).

[6] W. Miller, *Symmetry Groups and their Applications*, Academic Press, Chap. 4, 1972.

[7] R.P. Feynman, A.R. Hibbs, *Quantum Mechanics and Path Integral*, McGraw-Hill, 1965.

[8] G. Roepstorff, *Path Integral Approach to Quantum Physics*, Springer, 1994.

[9] V. Ballenegger, Ph.A. Martin, A. Alastuey, *J. Stat. Phys.* **112**, 169 (2002).

[10] F. Cornu, *Phys. Rev.* **E53**, 5595, 1996 and *Phys. Rev.* **E58**, 5268 (1998).

[11] F. Cornu, *Phys. Rev. Lett.* **78**, 1464 (1997).

[12] A. Alastuey, V. Ballenegger, F. Cornu and Ph. A. Martin, Screened cluster expansion for partially ionized gases, `cond-mat/0304059`, to be published in *J. Stat. Phys.* (2003) and Equation of state of the hydrogen plasma in the atomic limit: asymptotic estimations of non-ideal contributions at low temperature, preprint ENS (Lyon) and EPFL (Lausanne) (2003); V. Ballenegger, Ph. A. Martin, `cond-mat/0304061`, Dielectric versus conductive behaviour in quantum gases: exact results for the hydrogen plasma, submitted to *Physica A* (2003).

[13] F. Dalfovo, S. Giorgini, S. Stringari, L. Pitaevskii, *Rev. Mod. Phys.* **71**, 463 (1999).

[14] J.L. Lebowitz, O. Penrose, *J. Math. Phys.* **7**, 68 (1966).

[15] K. Huang, *Statistical Mechanics*, John Wiley, 1963.

[16] J.T. Lewis, *Lecture Notes in Physics* **257**, 234 (1986).

[17] J.T. Lewis, J.T. Pulé, Ph. de Smedt, The persistence of boson condensation in the van der Waals limit, Dublin Institute for Advanced Studies, STP-83-48 (1983).

[18] Ph. de Smedt, V. Zagrebnov, *Phys. Rev.* **A35**, 4763 (1987).

[19] Ph.A. Martin, J. Piasecki, Quantum Mayer graph analysis of the Bose gas, `cond-mat/0304392`, to be published in *Phys. Rev.* **E** (2003).

[20] B. Duplantier, *Nucl. Phys.* **B430**, 489 (1994).